Biochimica et Biophysica Acta 1818 (2012) 861–868

Contents lists available at SciVerse ScienceDirect

Biochimica et Biophysica Acta

journal homepage: www.elsevier.com/locate/bbamem

Structural investigation of the transmembrane C domain of the mannitol permease from *Escherichia coli* using 5-FTrp fluorescence spectroscopy

Milena Opačić [a], Ben H. Hesp [b], Fabrizia Fusetti [c], Bauke W. Dijkstra [a], Jaap Broos [a,*]

[a] Laboratory of Biophysical Chemistry, Groningen Biomolecular Sciences and Biotechnology Institute, University of Groningen, Nijenborgh 7, 9747 AG Groningen, The Netherlands
[b] Zernike Institute for Advanced Materials, University of Groningen, Nijenborgh 4, 9747 AG Groningen, The Netherlands
[c] Department of Biochemistry, Netherlands Proteomics Centre, University of Groningen, Nijenborgh 4, 9747 AG Groningen, The Netherlands

ARTICLE INFO

Article history:
Received 8 July 2011
Received in revised form 1 October 2011
Accepted 2 November 2011
Available online 9 November 2011

Keywords:
Anisotropy
Fluorotryptophan
Iodide quenching
Membrane protein
PTS
Time-resolved fluorescence spectroscopy

ABSTRACT

The mannitol transporter EII^{mtl} from *Escherichia coli* is responsible for the uptake of mannitol over the inner membrane and its concomitant phosphorylation. EII^{mtl} is functional as a dimer and its membrane-embedded C domain, IIC^{mtl}, harbors one high affinity mannitol binding site. To characterize this domain in more detail the microenvironments of thirteen residue positions were explored by 5-fluorotryptophan (5-FTrp) fluorescence spectroscopy. Because of the simpler photophysics of 5-FTrp compared to Trp, one can distinguish between the two 5-FTrp probes present in dimeric IIC^{mtl}. At many labeled positions, the microenvironment of the 5-FTrps in the two protomers differs. Spectroscopic properties of three mutants labeled at positions 198, 251, and 260 show that two conserved motifs (Asn194-His195 and Gly254-Ile255-His256-Glu257) are located in well-structured parts of IIC^{mtl}. Mannitol binding has a large impact on the structure around position 198, while only minor changes are induced at positions 251 and 260. Phosphorylation of the cytoplasmic B domain of EII^{mtl} is sensed by 5-FTrp at positions 30, 42, 251 and 260. We conclude that many parts of the IIC^{mtl} structure are involved in the sugar translocation. The structure of EII^{mtl}, as investigated in this work, differs from the recently solved structure of a IIC protein transporting diacetylchitobiose, ChbC, and also belonging to the glucose superfamily of EII sugar transporters. In EII^{mtl}, the sugar binding site is more close to the periplasmic face and the structure of the 2 protomers in the dimer is different, while both protomers in the ChbC dimer are essentially the same.

1. Introduction

The EII sugar transporters of the bacterial-specific phospho*enol*pyruvate (PEP) dependent phosphotransferase system (PTS) phosphorylate their cognate substrates during transport over the membrane. EII transporters belong to the class of group translocation transporters, which is distinct from the classes of primary and secondary transporters [1]. The D-mannitol specific mannitol permease from *Escherichia coli*, EII^{mtl}, is one of the best-characterized EII sugar transporters [2]. It is a 68-kDa protein composed of three covalently linked domains, two cytoplasmic domains, A and B, and a membrane-embedded C domain (IIC^{mtl}). It transports mannitol from the periplasm to the cytoplasm, where it is released as mannitol-1-phosphate [2,3]. The phosphoryl group originates from PEP and is delivered to mannitol in the C domain *via* His^{554} in the A domain and Cys^{384} in the B domain of EII^{mtl}, respectively. The structures of the A and the B domains have been solved by X-ray crystallography and NMR spectroscopy [4,5]. For the membrane-embedded IIC^{mtl} (346 residues), which harbors the mannitol translocation pathway, a 2D projection map at 5 Å resolution is available [6]. EII^{mtl} is functional as a dimer and it contains one high-affinity mannitol binding site per dimer [7].

Various biophysical and biochemical approaches, including Trp fluorescence spectroscopy, have been exploited to study mechanistic and structural features of EII^{mtl} [8–11]. WT EII^{mtl} contains four Trp residues, all located in the C domain but they can be replaced by Phe residues without significant loss of function [8]. This mutant protein was used to construct single Trp mutants of EII^{mtl} [12,13]. Recently, 5-fluoroTrp (5-FTrp), which displays much more homogeneous fluorescence decay kinetics than Trp [14–16], was biosynthetically incorporated into these mutants. In favorable cases, one can distinguish between the two fluorophores present per dimer and it was found that dimeric EII^{mtl} does not form a symmetric dimer [11]. Förster resonance energy transfer (FRET) measurements carried out with 19 single Trp mutants of EII^{mtl}, where 5-FTrp was the donor and the substrate analogue azi-mannitol the acceptor, indicated that the mannitol binding site is

Abbreviations: EII^{mtl}, the mannitol-specific transporting and phosphorylating enzyme from *E. coli*; IIC^{mtl}, membrane-embedded C domain of EII^{mtl}; Trp, tryptophan; 5-FTrp, 5-fluorotryptophan; TOE, tryptophan octyl ester: mannitol, D-mannitol; FRET, Förster resonance energy transfer; FWHH, full width at the half height; ϕ, rotational correlation time; NATA, N-acetyl-tryptophanamide; PEG, Polyethylene glycol

* Corresponding author. Tel.: +31 50 3634277; fax: +31 50 3634800.
E-mail address: J.Broos@rug.nl (J. Broos).

0005-2736/$ – see front matter © 2011 Elsevier B.V. All rights reserved.
doi:10.1016/j.bbamem.2011.11.001

Nomenclature

Trp-less EII^{mtl} indicates wt EII^{mtl} in which the four native Trps are replaced by Phe. W30, W38, W42, W66, W147, W167, W180, W188, W198, W251, W260, W282, and W327 are the single-Trp-containing EII^{mtl} mutants based on Trp-less EII^{mtl}.
W30 C384S, W42 C384S, W251 C384S, and W260 C384S are the single-Trp-containing EII^{mtl} mutants based on Trp-less EII^{mtl} carrying a Cys384Ser mutation.

asymmetrically positioned in the dimer [12]. Residue positions 30, 38, 97, 133 were found at 7–8 Å from the mannitol-binding site. Furthermore, experiments with stably phosphorylated mutants showed that this site is also the site where mannitol becomes phosphorylated.

Here we characterize 13 positions in the C-domain of EII^{mtl} by 5-FTrp fluorescence spectroscopy, including two native Trp positions at 30 and 42. Conservative Phe→Trp and Tyr→Trp mutations were introduced in Trp-less EII^{mtl} at positions spread through the C domain (positions 66, 147, 167, 180, 188, 198, 251, 260, 282, and 327). Ile38, close to the mannitol binding site was also mutated to Trp. Characterization of these mutants in absence and presence of mannitol informs which parts of IIC^{mtl} are involved in the mannitol transport process and the 5-FTrp spectroscopy approach can also elucidate structural differences between the two protomers in dimeric EII^{mtl}. Recently, it was reported that mutants containing the C384S mutation in the B domain become irreversibly phosphorylated at Ser384, mimicking therefore the activated form of the enzyme [17,18]. Here 5-FTrp fluorescence spectroscopy is used to investigate if the IIC^{mtl} structure near positions 30, 42, 251, and 260 is affected by B domain phosphorylation. Positions 30 and 42 are close to the mannitol binding site while positions 251 and 260 flank the conserved GIXE motif (Gly254-Ile255-His256-Glu257). The presented data provide structural details of EII^{mtl} near the 5-FTrp labeled positions and the impact of mannitol binding and B domain phosphorylation on this. Moreover, the data informs at which 5-FTrp labeled positions the two protomers in dimeric EII^{mtl} differ in structure. In the course of this work, the first 3D structure of a IIC domain was presented, the diacetylchitobiose transporter, ChbC, from *Bacillus cereus* [19]. Comparison of the structural features of EII^{mtl} with the ChbC structure shows the single high affinity mannitol binding site in EII^{mtl} is located more close to the periplasmic face than the two binding sites present in ChbC, both binding diacetylchitobiose. Another clear difference is that both protomers in dimeric EII^{mtl} differ in structure while in dimeric ChbC the structure of both protomers are essentially the same.

2. Materials and methods

2.1. Chemicals and reagents

$C_{10}E_5$ detergent was obtained from Kwant High Vacuum Oil Recycling and Synthesis, Bedum, The Netherlands, and fluorescent impurities were removed as described [20]. KI (Suprapur) was from Merck. N-decyl-β-D-maltoside (DM) was from Anatrace.

2.2. EII^{mtl} mutants

The construction of the single-Trp-containing mutants of EII^{mtl} used in this work have been described before [12,13,21]. Briefly, all single Trp mutants, except W38, were based on Trp- less EII^{mtl} with a N-terminal His_6 tag [13] while mutant W38 is based on Trp- less EII^{mtl} with a C-terminal His_6 tag [12]. Trp codons were introduced using the QuickChange site-directed mutagenesis kit of Stratagene. The nonvectorial phosphorylation activities and the mannitol dissociation constants (K_Ds) of the mutants have been reported before [8,12,21]. The nonvectorial phosphorylation activities of the investigated mutants varied from 65% of the WT EII^{mtl} activity (mutants W180 and W282) to 15% in the case of mutants W251 and W327 [7]. As expected, mutants containing the C384S mutation were inactive [22]. The C384S mutation does not affect the K_D of mannitol [23]. The K_Ds of the mutants are presented in Table S1.

Biosynthetic incorporation of 5-FTrp in the single Trp mutants of EII^{mtl} was according to a published procedure [24]. This procedure results in over 95% incorporation of 5-FTrp at a Trp codon position [24]. In-side-out vesicles were prepared as described [10]. EII^{mtl} mutants were purified using a two-step purification procedure [11]. The C384S mutants were first phosphorylated and subsequently purified as described [12]. Mass spectrometry analysis showed that this procedure resulted in complete phosphorylation of Ser384 in these mutants [12]. For this analysis, the purified C384S mutant was treated with trypsin and analyzed by nano-flow reversed-phase high performance liquid chromatography (RP-HPLC) tandem mass spectrometry (MS/MS) on a linear quadrupole ion trap-Fourier transform hybrid mass spectrometer (LTQ Orbitrap XL). The 380–390 peptide was detected exclusively in the phosphorylated form, with a deviation of 0.003 Da from the theoretical mass. MS/MS experiments identified Ser384 as the phosphorylation site.

2.3. Fluorescence experiments

All fluorescence spectroscopy measurements were performed in buffer containing 20 mM Tris, pH 8.4, 1 mM reduced glutathione, 250 mM NaCl and 0.25% (*v*/*v*) $C_{10}E_5$. In this optimized buffer system, EII^{mtl} is present as dimers [2] and the specific mannitol phosphorylation activity of purified wt EII^{mtl} is only 10–20% lower compared to the unpurified protein in *E. coli* membrane vesicles [7,25]. For steady state fluorescence measurements a Fluorolog3-22 spectrofluorometer (Jovin Yvon) was used. The excitation wavelength was 295 nm and the emission was measured from 305 to 500 nm. The excitation and emission slit widths were 1.25 and 4 nm respectively, and the temperature was 23 °C. All spectra were recorded at least twice and were corrected for background emission and instrument response. The emission intensities presented in Stern–Volmer (S–V) plots were calculated using the integrated area of the emission peaks between 305 and 460 nm. If both 5-FTrp residues show a similar solvent accessibility towards KI, a linear Stern–Volmer (S–V) dependence is expected. If the solvent-accessibility of the two 5-FTrp probes is not the same, an S–V plot, featuring a downward curvature, is obtained [26]. KI and not acrylamide was used as quencher because the latter likely partitions into the $C_{10}E_5$ belt surrounding EII^{mtl}, in this way biasing the quenching data. Moreover, acrylamide can quench the singlet Trp state quite efficiently via a through space mechanism [27].

Time resolved fluorescence spectroscopy measurements were performed at 20 °C as described elsewhere [11]. The excitation wavelength was 305 nm and a 368 nm interference filter (IF) with a 17 nm full width at half height (FWHM) band-pass (Schott) was used. In time-correlated single photon counting measurements, where excitation was at 295 nm, a 349 nm IF with a 8 nm FWHH band pass filter and a cut-off filter (WG320, Schott) were used to collect the emission [14]. An excitation wavelength of 295 nm was used for mutants

exhibiting a very blue emission like W180, W327, and W198. Excitation at 295 nm made it possible to collect a strong emission signal using this filter without the interference of the water Raman signal. Despite the low intrinsic anisotropy (r_0) value upon excitation at 295 nm ($r_0 = 0.1$), it was possible to observe changes in anisotropy upon mannitol binding (Table 3, Fig. S4 in the Supplementary data). Data were analyzed with a model of discrete exponentials using the TRFA data processing package, version 1.2, of SSTC, Belarusian State University, Belarus.

3. Results

Thirteen single Trp mutants of EII^{mtl} labeled with 5-FTrp at positions 30, 38, 42, 66, 147, 167, 180, 188, 198, 251, 260, 282 and 327 (mutants W30, W38, W42, W66, W147, W167, W180, W188, W198, W251, W260, W282 and W327, respectively), together with four mutants containing an additional C384S mutation (mutants W30 C384S, W42 C384S, W251 C384S, and W260 C384S), were investigated. In the C384S mutants, S384 can be stably phosphorylated, in this way mimicking EII^{mtl} in its phosphorylated state [17]. All 5-FTrp labeled positions are in the C domain of EII^{mtl}.

3.1. Emission spectra in the absence and presence of mannitol

The maxima (λ^{max}) of the steady state emission spectra of all seventeen studied mutants are presented in Table 1. Typically, spectra of proteins containing 5-FTrp are 7 nm red-shifted compared to the same protein containing Trp [15]. All mutants show a λ^{max} within a narrow range between 320 and 335 nm, λ^{max} values significantly bluer than the λ^{max} for free 5-FTrp (354 nm) in aqueous buffer [15] or for 5-FTrp embedded in $C_{10}E_5$ micelles (~340 nm, see Supplementary material). Thus the 5-FTrp side chains at all studied positions are not fully surface exposed.

Mannitol binding influenced the emission intensities of six of the studied positions (Table 1). We note that 5-FTrp is less sensitive for monitoring conformational changes as its quantum yield is affected to only a minor degree by electron transfer to nearby acceptor sites (e.g. peptide bonds) [15]. For example, the fluorescence intensity of mutant W30 increases 13% upon mannitol binding [8], but when position 30 is labeled with 5-FTrp the change is only −4%. W198 was the only mutant studied in this work that showed a significant, 13 nm blue shift of λ^{max} upon mannitol binding (Table 1, Fig. 1A).

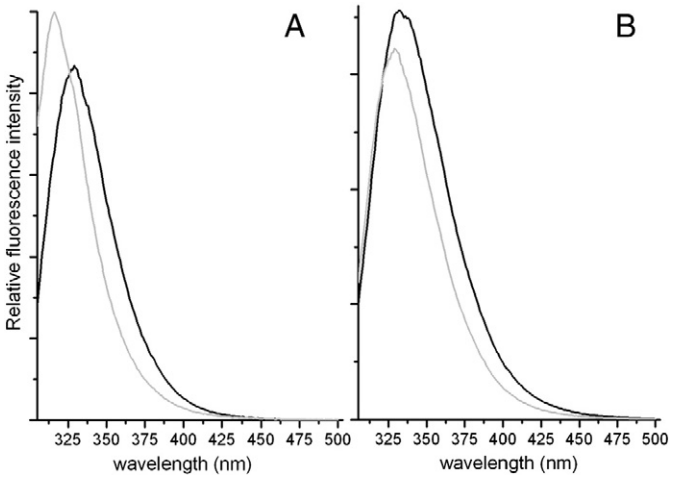

Fig. 1. (A) The emission spectrum of mutant W198 in absence (black) and presence of 50 μM mannitol (gray). (B) The emission spectrum of mutant W188 in absence of KI (black), and in presence of 235 mM KI (gray).

The λ^{max} of W198 + mannitol (316 nm) is exceptional blue for 5-FTrp in a protein [15] and is the bluest λ^{max} reported to date.

3.2. Solvent accessibility of the different 5-FTrp positions

KI was used as a dynamic quencher to probe the solvent accessibility of the two 5-FTrp positions in the dimeric EII^{mtl} protein. The $C_{10}E_5$ detergent belt around EII^{mtl} may affect the solvent-accessibility of 5-FTrp but Stern–Volmer (S–V) experiments with the hydrophobic tryptophan derivative tryptophan octyl ester (TOE) [28] showed that the presence of $C_{10}E_5$ has only a small impact on the EII^{mtl} iodide quenching data (see Supplementary material).

The emission of mutant W167 was found most sensitive for KI. A linear S–V relationship was obtained, both in the absence and presence of mannitol, with S–V constant (K_{sv}) values of 3.9 M^{-1} and 4.8 M^{-1}, respectively (Fig. 4). The τ_{av} values ($\tau_{av} = \Sigma\ \alpha_i\tau_i$) of this mutant are 4.0 ns without mannitol and 3.7 ns in the presence of mannitol, yielding collisional quenching constant (k_q) values of 1.0×10^9 M^{-1} s^{-1} and 1.3×10^9 M^{-1} s^{-1}, respectively. These values are 1.9 and 1.5 times lower than the k_q of TOE in $C_{10}E_5$ micelles under

Table 1
Fluorescence emission properties of 5-FTrp-containing mutants of EII^{mtl}.

Mutant	λ_{max} (nm)	Emission intensity change + 50 μM mannitol (%)
W30	323	−4
W30 C384S	323	−2
W38	332	0
W42	331	+6
W42 C384S	330	+3
W66	335	0
W147	333	0
W167	331	0
W180	320	0
W188	333	0
W198	329	+16 [a] (λ_{max} = 316 nm)
W251	326	+7
W251 C384S	325	+3
W260	328	0
W260 C384S	332	−6
W282	327	0
W327	320	+5

[a] The integrated area from 329 nm to 450 nm (without mannitol) was compared to the integrated area from 316 nm to 450 nm (+ mannitol).

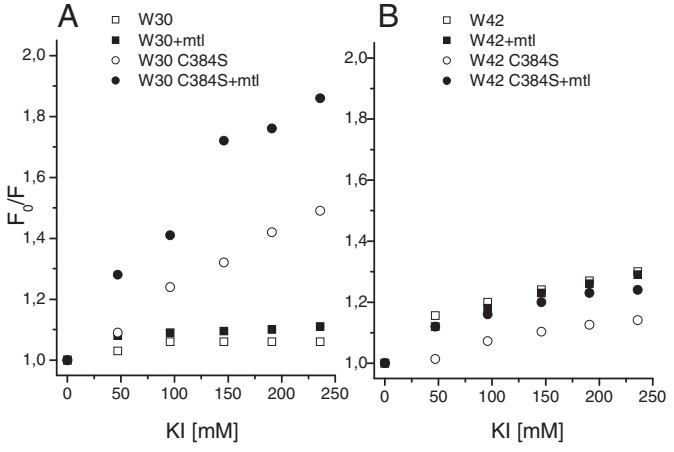

Fig. 2. Stern-Volmer plots of EII^{mtl} mutants with KI as quencher.Panel A: W30 (□); W30 in presence of 50 μM mannitol (■); W30 C384S (○); and W30 C384S in presence of 50 μM mannitol (●).Panel B: W42 (□), W42 in presence of 50 μM mannitol (■); W42 C384S (○); and W42 C384S in presence of 50 μM mannitol (●).

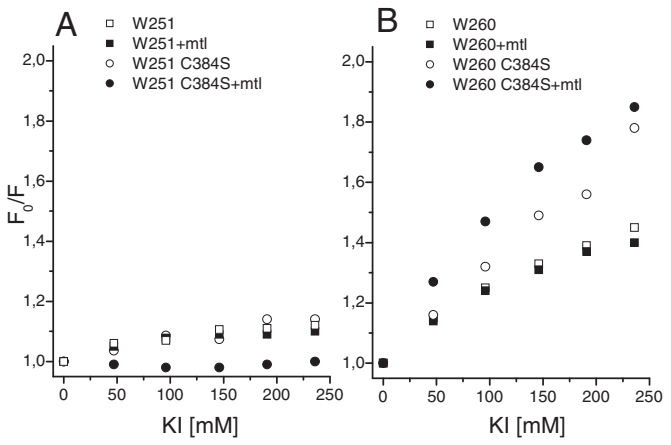

Fig. 3. Stern-Volmer plots of EII^{mtl} mutants with KI as quencher. Panel A: W251 (□); W251 in presence of 50 μM mannitol (■); W251 C384S (○); and W251 C384S in presence of 50 μM mannitol (●). Panel B: W260 (□); W260 in presence of 50 μM mannitol (■); W260 C384S (○); and W260 C384S in presence of 50 μM mannitol (●).

the same conditions (Fig. S1). Likely position 167 is located close to the protein surface at a structured position as also a blue λ^{max} was observed and a low rotational mobility (see below). The linear S–V relationship demonstrates that the accessibility is similar for both EII^{mtl} proteomers.

Also for mutants W30 C384S and W260 C384S, linear S–V plots were obtained (Figs. 2, 3), yielding $k_q s$ of $0.5\times10^9\,M^{-1}\,s^{-1}$ and $0.8\times10^9\,M^{-1}\,s^{-1}$ respectively, 3.8 and 2.4 times lower than the k_q of TOE in $C_{10}E_5$ micelles. A modest solvent accessibility, and 20–35% quenching with up to 240 mM KI, was observed for mutants W38, W42, W198, and W260 (Figs. 2–4). The fluorescence emission of the remaining mutants was quenched less than 20% when up to 240 mM KI was present. By and large, the majority of the studied residue positions are shielded from the solvent.

In the case of W188 (Fig. 1B), W198, and W260, addition of increasing concentrations of KI resulted in quenching of the red part of the spectrum while the emission at the blue part was minimally affected. Thus, in these mutants, the two 5-FTrp probes present per dimer emit at different wavelengths and the red emitting 5-FTrp is more solvent accessible than the blue emitting one. For the other mutants, no clear changes in the position of λ^{max} were visible during the KI titration.

3.3. Structural differences between the two proteomers in EII^{mtl} mutants

Time-resolved fluorescence experiments were conducted to investigate if structural differences exist between the two protomers in dimeric EII^{mtl}. If both 5-FTrp probes in the dimer are embedded in a similar microenvironment, a monoexponential decay is expected while structural differences at a site result in a multiexponential decay.

The fluorescence intensity decay spectra of all mutants are presented in Fig. S3, together with the reduced residuals and the corresponding autocorrelation function of the used fit functions. The obtained fit parameters are presented in Table 2. On the basis of their decay kinetics, the studied mutants can be divided in three categories. (i) Mutants with an essentially homogeneous decay with the fraction of the main component (α) between 1.0 and 0.8 (W30, W30 C384S, W42, W42 C384S, W147, W180, W251, and W251 C384S), (ii) Mutants with a biexponential decay ($\alpha_1 \approx \alpha_2$) (W38, W188, W198, W282 and W327), and (iii) Mutants exhibiting heterogeneous decays (W66, W167, W260 and W260 C384S) (Table 2). Mannitol binding induced an increase in lifetime heterogeneity for W42 and W42 C384S with the decay changed to a biexponential decay ($\alpha_1 \approx \alpha_2$), while that of W147 changed to heterogeneous decay. Thus mannitol binding results in structural differences between the two protomers at positions 42 and 147. In summary, the time-resolved fluorescence decay analysis of the 5-FTrp labeled EII^{mtl} mutants clearly indicate that the structure of the two protomers in dimeric EII^{mtl} is different at many residue positions investigated.

3.4. Rotational mobility of the 5-FTrp side chains in EII^{mtl} mutants

To probe the rotational mobility of the 5-FTrp side chains, time resolved anisotropy decays were determined (Fig. S4). The anisotropy decay of each mutant is dominated by 5-FTrp immobile at the fluorescence decay lifetime scale (rotational correlation time (ϕ) = ∞ ns, $\equiv \geq 10\times\tau$) (Table 3). ϕ values between 0.1 and 10 ns are also present and could be a result of wobbling [26], or homoenergy transfer between the two 5-FTrp residues in the dimer [16]. A control experiment with TOE in $C_{10}E_5$ showed that the detergent minimally affects the rotational mobility of the indole side chain (Fig. S2B). The long ϕ values are therefore caused by the protein matrix surrounding the 5-FTrp probe. Mutant W66 gave an associated anisotropy decay curve [26] (Figs. 5, S4), which shows that this sample contains a population of emitting molecules with short τ and short ϕ, as well as a population with long τ and long ϕ. This results in a minimum in anisotropy after a short time and a subsequent increase of the anisotropy after longer times. This is a clear indication of structural differences between the two 5-FTrp residues in dimeric W66.

Addition of mannitol had a notable influence on the rotational mobility of all 5-FTrp positions investigated, except for mutants W30 C384S, W38, W251, W260 C384S and W327 (Table 3, Fig. S4). Thus, a large fraction of the residue positions studied is affected by mannitol binding. However, all residues retain a low rotational mobility, suggesting that they all remain in a well-structured region of the protein.

4. Discussion

In this work we investigated the microenvironment of thirteen positions in IIC^{mtl} using 5-FTrp-fluorescence spectroscopy. Our data reveal structural features of IIC^{mtl} near two conserved motifs, Asn194-His195 and Gly254-Ile255-His256-Glu257, it informs about the effect of B domain phosphorylation and mannitol binding on the IIC^{mtl} structure, and it probes differences between the two protomers in dimeric IIC^{mtl}. These features of EII^{mtl} are discussed below and compared with the X-ray structure of the diacetylchitobiose transporter, ChbC, from *Bacillus cereus* [19].

4.1. Structure of IIC^{mtl} at regions critical for the EII^{mtl} activity: the GIXE motif and the region near Asn194 and His195

Extensive mutagenesis studies of the IIC^{mtl} domain over the years have resulted in relatively few residue positions that were found to be essential for EII^{mtl} activity [29–33]. Critical positions include the GIXE motif (residues 254–257), and residue positions 194–195 [34]. The GIXE motif is highly conserved among all known EIIs with the glutamate (E) fully conserved [35]. Several studies have pointed out that both motifs in EII^{mtl} are most likely involved in phosphate and/or substrate binding [29–32,34]. Structural features of IIC^{mtl} surrounding these motifs in EII^{mtl} have not been reported. As mutagenesis of these conserved residues resulted in proteins not being able to bind mannitol any longer, Trp residues were introduced at flanking positions (198, 251, 260) to study this important part of EII^{mtl}. Trp198 was found 13 Å away from the mannitol binding site while Trp251 and Trp260 are 15–16 Å from this site [12].

W251 and W260 show blue emission maxima, characteristic of residues in a hydrophobic environment. The 5-FTrps in these mutants show a modest (W260) to very low (W251) accessibility for KI as dynamic quencher (Fig. 3). The anisotropy decays of both

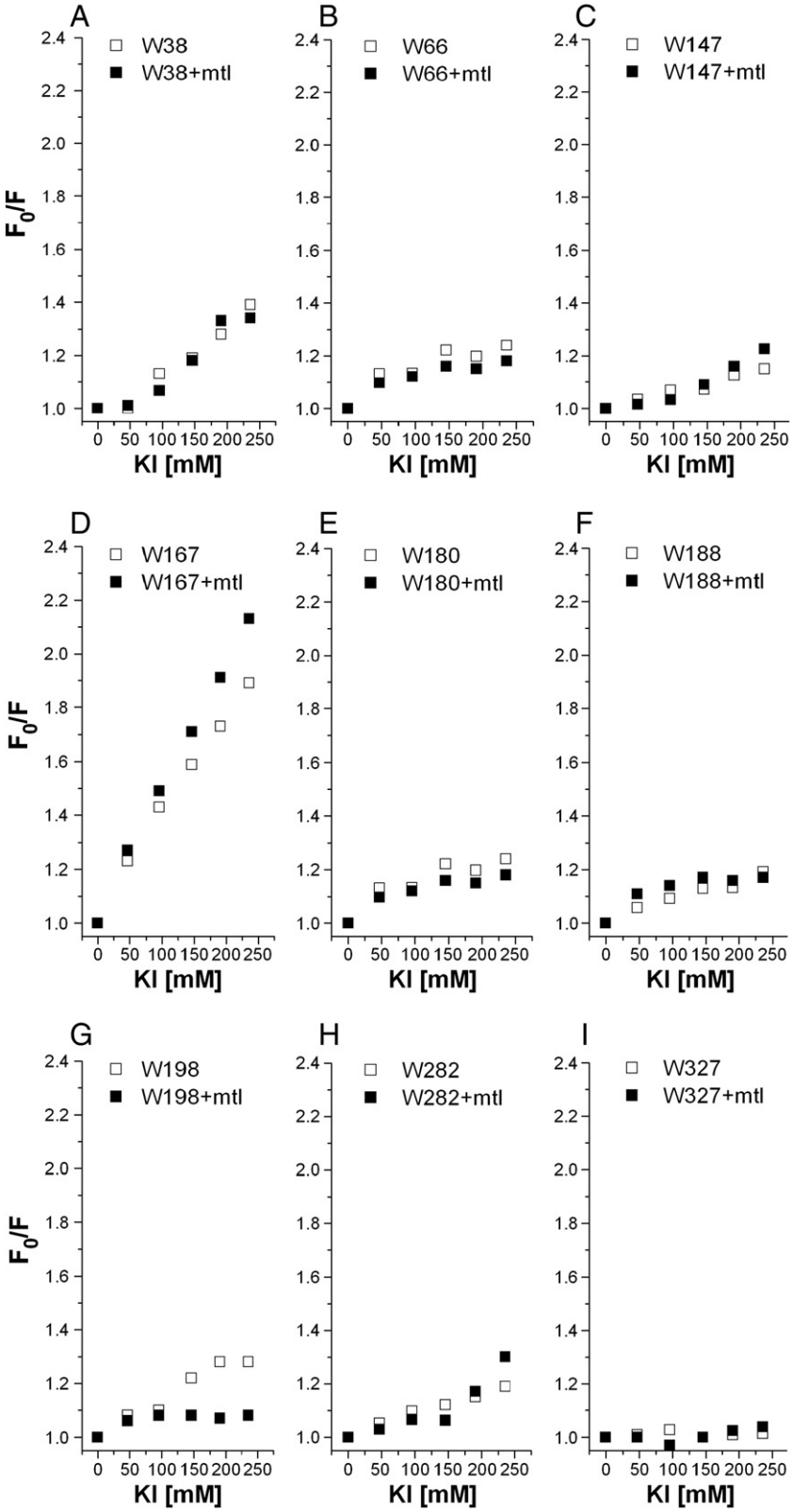

Fig. 4. Stern-Volmer plots of EII^{mtl} mutants with KI as quencher. A) W38; B)W66; C) W147; D) W167; E W180; F) W188; G) W198; H)W282 M) ; and I) W327 in absence (□) and in presence of 50 μM mannitol (■).

residues are dominated by a large fraction of 5-FTrp immobilized on the nanosecond timescale. Taken together, these data demonstrate that IIC^{mtl} is well structured around these two positions. Upon mannitol binding only small changes in the anisotropy decays were observed, as well as only small changes in the solvent accessibility of these sites. Thus, mannitol binding does not induce major structural rearrangements near the GIXE motif.

The fluorescence properties of mutant W198 are also typical for a 5-FTrp at a buried position. Addition of mannitol to W198 results in a significant increase in emission intensity, as well as a large, 13 nm

Table 2
Time resolved fluorescence intensity decay parameters of single 5-FTrp containing mutants of EII^{mtl} in the absence and presence of 50 μM mannitol[a].

Mutant	τ_1 (ns)	τ_2 (ns)	τ_3 (ns)	τ_4 (ns)	α_1	α_2	α_3	α_4	χ^2
W30	4.4	1.1			95	5			1.07
+ mtl	4.5	1.9			95	5			0.98
W30 C384S	7.2	4.3			5	95			1.06
+ mtl	7.7	4.3			4	96			1.06
W38	5.4	4.0	1.0		45	50	5		1.02
+ mtl	5.3	3.8	0.6		48	44	7		1.10
W42	4.8	2.4			81	19			1.08
+ mtl	5.3	3.9	0.8		51	47	2		1.11
W42 C384S	4.9	2.6			77	23			1.05
+ mtl	5.4	4.0	0.7		51	46	3		1.11
W66	5.2	2.8	1.0	0.2	13	29	30	28	1.05
+ mtl	5.5	2.5	0.6	0.1	11	32	27	30	0.98
W147	5.0								1.00
+ mtl	5.9	4.6	0.3		26	69	5		1.10
W167	4.7	2.1			72	28			1.10
+ mtl	5.9	3.9	1.3		18	62	20		1.03
W180	5.0								1.03
+ mtl	5.0	2.0			97	3			1.13
W188	5.8	4.1	1.3		47	50	3		1.00
+ mtl	5.8	4.0			50	50			1.05
W198	4.9	4.1			50	50			1.03
+ mtl	5.7	4.2			50	50			1.07
W251	4.4								1.01
+ mtl	4.3	2.1			97	3			1.00
W251 C384S	4.5	2.5			94	6			1.05
+ mtl	4.4	2.6			92	8			1.08
W260	4.8	2.1	0.3		63	20	17		1.02
+ mtl	4.9	2.1	0.3		68	12	20		1.10
W260 C384S	6.4	4.0	1.1		20	68	12		1.04
+ mtl	7.0	4.1	1.2		14	72	14		1.07
W282	4.6	3.9	3.0		48	49	3		1.00
+ mtl	4.9	3.6			50	50			1.06
W327	5.1	3.6			50	50			1.09
+ mtl	5.1	3.6			50	50			1.15

[a] The total intensity was assumed as $I(t) = \Sigma_i \alpha_i \exp(-t/\tau_i)$ with $\Sigma_i \alpha_i = 100$.

Table 3
Time resolved fluorescence anisotropy decay parameters of single 5-FTrp containing mutants of EII^{mtl} in the absence and presence of 50 μM mannitol[a].

Mutant	ϕ_1 (ns)	ϕ_2 (ns)	ϕ_3 (ns)	ϕ_4 (ns)	β_1	β_2	β_3	β_4	χ^2
W30	11.8	0.58	0.03		0.04	0.02	0.06		1.00
+ mtl	∞	1.33	0.04		0.07	0.02	0.04		0.98
W30 C384S	16.2	0.26	<0.01		0.04	0.02	0.05		1.05
+ mtl	∞	16.3	0.27		0.08	0.03	0.03		1.05
W38	∞	0.38			0.18	0.02			1.05
+ mtl	∞	0.16			0.18	0.02			1.07
W42	∞	6.70	0.36		0.08	0.06	0.04		1.04
+ mtl	34.0	1.70	0.06		0.12	0.04	0.05		1.06
W42 C384S	∞	6.80	0.77		0.10	0.02	0.04		1.07
+ mtl	40.0	1.40	0.01		0.11	0.06	0.10		1.09
W66	33.0	1.00	0.06	<0.01	0.09	0.02	0.07	0.06	1.02
+ mtl	26.0	1.50	0.02		0.09	0.07	0.15		0.98
W147	∞	5.10	0.18		0.10	0.04	0.03		0.97
+ mtl	∞	1.80	0.04		0.12	0.03	0.05		1.06
W167	∞	0.66	0.02		0.16	0.03	0.03		1.06
+ mtl	45.0	0.56	0.08		0.16	0.02	0.03		1.03
W180	∞	7.50	0.18		0.07	0.03	0.07		1.05
+ mtl	∞	0.60			0.10	0.02			1.07
W188	∞	9.50	0.35		0.08	0.06	0.03		1.02
+ mtl	∞	1.20	0.11		0.12	0.04	0.03		1.04
W198	∞	9.40			0.10	0.02			1.05
+ mtl	∞	1.11			0.08	0.02			1.04
W251	∞	1.50	0.01		0.19	0.03	0.07		1.00
+ mtl	∞	0.17			0.19	0.02			1.02
W251 C384S	∞	3.10	0.18		0.20	0.04	0.02		0.98
+ mtl	∞	0.66	0.06		0.20	0.03	0.03		1.06
W260	∞	3.70	0.07		0.13	0.03	0.09		1.05
+ mtl	∞	0.77	0.08		0.14	0.02	0.05		1.04
W260 C384S	∞	5.30	0.53		0.10	0.06	0.03		1.06
+ mtl	∞	5.20	0.34		0.10	0.06	0.04		1.04
W282	∞	3.50	0.25		0.06	0.03	0.03		1.00
+ mtl	33.0	1.04	0.12		0.07	0.04	0.04		1.06
W327	19.0	2.40			0.07	0.03			1.03
+ mtl	15.0	1.20			0.08	0.02			1.10

[a] The anisotropy decay was assumed as $r(t) = \Sigma_i \beta_i \exp(-t/\phi_i)$, $r(0) = \Sigma_i \beta_i$, $\phi = \infty$ corresponds with $\phi > 10 \times \tau$.

blue shift to 316 nm (Fig. 1A). This blue shift induced upon mannitol binding is indicative of a large conformational change near residue 198 [36]. KI quenching data for this mutant demonstrate 5-FTrp at 198 becomes more buried upon mannitol binding (Fig. 4). Taken together, this work shows for the first time that the region near conserved residues 194–195 is embedded in a structured and occluded part of IIC^{mtl}, but is sensitive to binding of mannitol.

Recently, the first 3D structure of a IIC protein, the N, N′-diacetylchitobiose transporter from *Bacillus cereus* (ChbC), was reported [19]. Like EII^{mtl}, ChbC belongs to the Glc superfamily of PTS sugar permeases and members of this superfamily are expected to have structural and topological features in common [35]. The X-ray structure shows a homodimeric protein and each protomer binds a diacetylchitobiose sugar molecule at a binding site oriented towards the cytoplasmic face. Residues Glu334 and His250, corresponding to Glu257 and His195 in EII^{mtl} [19], make H-bonds with the C6 hydroxyl group of the sugar which is phosphorylated, suggesting that residues of both conserved motifs are involved in sugar phosphorylation. The authors propose that for release of the sugar to the cytoplasm a relative small conformational change is needed, the movement of a loop from the neighboring protomer, but that for binding of the sugar at the periplasmic side, a larger conformational change is needed. In the ChbC structure, the residues corresponding to 5-FTrp in EII^{mtl} mutants W251, and W260, are close to the sugar while in EII^{mtl}, at conditions studied in this work, these 5-FTrp residues are 15–16 Å from where mannitol binds [12]. In contrast, 5-FTrps in EII^{mtl} mutants W30, W38, W97, and W133 were found close (7–8 Å) to where mannitol binds while the corresponding residues in ChbC are at the periplasmic face and > 25 Å away from the sugar. This shows that, at the conditions used in this work, the sugar binding site in EII^{mtl} is more towards the periplasmic face that in the ChbC structure, suggesting the two proteins are in different conformational states. Dimeric EII^{mtl} harbors only one high affinity mannitol binding site (K_D ~ 100 nM), and the presence of a second "resting" site has been proposed [12]. A K_D < 0.1 mM could be excluded

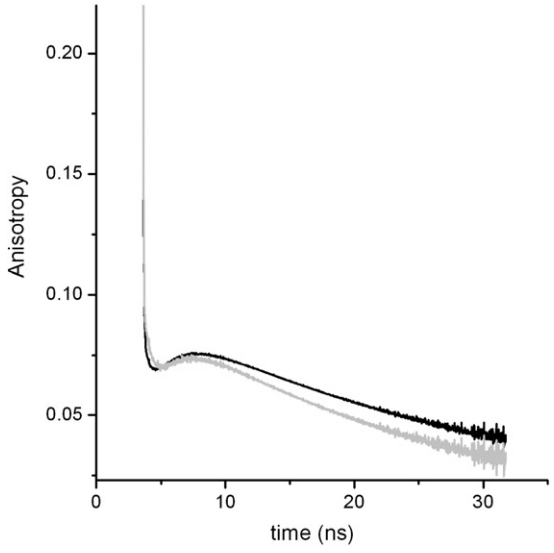

Fig. 5. Anisotropy decay of EII^{mtl} mutant W66 in absence (black) and presence (gray) of 50 μM mannitol.

for this second binding site [7]. ChbC was crystallized in the presence of 4 mM diacetylchitobiose and two sugars are bound per dimer. Thus EII^{mtl} as studied in this work is in a different stage of the transport cycle than the ChbC structure.

4.2. Conformational changes induced in IIC^{mtl} upon mannitol binding and phosphorylation of the B domain

Changes in λ^{max}, emission intensity, KI quenching, lifetime and anisotropy upon mannitol binding are the largest for mutant W198 and mutants having the 5-FTrp close to the mannitol binding site like W30 and W42. In the case of W147 and W167, mannitol binding does not induce a notable change in λ^{max} and emission intensity, induces only small changes in KI quenching but the changes in lifetime are relatively large, demonstrating that dimeric EII^{mtl} undergoes structural changes at these sites, known to be > 16 Å away from the mannitol binding site [12].

EII^{mtl} has 2 cytoplasmic domains, A and B, and only the B domain is believed to directly interact with the membrane-embedded IIC^{mtl} [2]. Phosphorylation of EII^{mtl} at position Cys384 in the B domain accelerates mannitol transport by 2–3 orders of magnitude [37,38], demonstrating that a B/C inter-domain coupling is operative during sugar translocation. B domain phosphorylation induces docking of the B domain at the C domein, and brings the phosphoryl group to mannitol, bound at a central location in IIC^{mtl} [12]. Calorimetry studies showed 50 to 60 residues at the B/C interface to become buried upon B domain phosphorylation [39]. Knowledge on which parts of IIC^{mtl} interact with the B domain and/or change structure upon B domain phosphorylation is very limited. Cysteine accessibility studies showed that positions 85, 90 and 110 in IIC^{mtl} do sense B domain phosphorylation [40,41]. Here we have shown that also residues 30, 42, 251, and 260 sense phosphorylation of the B domain (Figs. 2, 3, S3, S4). Thus B domain phosphorylation induces conformational changes in the IIC^{mtl} structure flanking the GIXE motif at positions 251 and 260 and near the mannitol binding site at positions 30 and 42. The KI solvent-accessibilities of the 4 probed positions are not drastically reduced upon B domain phosphorylation (Figs. 2, 3), indicating that these positions are not at the B domain docking site. Remarkable is the result for position 42 which is facing the periplasm in the ChbC structure. This demonstrates that phosphorylation of the (cytoplasmic) B domain induces long range conformational changes in IIC^{mtl}.

As discussed in 4.1, the position of the sugar binding site in EII^{mtl} is close to the periplasmic face of IIC^{mtl}, while in ChbC, crystallized in the absence of the cytoplasmic A and B domains, the sugar is bound near the cytoplasmic face. Is this difference in sugar binding site position due to the presence of the cytoplasmic A and B domains in the EII^{mtl} mutants? In a published Trp phosphorescence study, the impact of the A and B domains on the IIC^{mtl} structure close to the sugar binding site has been investigated [21]. Mutant W97 and the truncated IIC^{mtl} version of this single Trp mutant (IIC^{mtl}-W97) were used in this study and characterized in absence and presence of mannitol. Position 97 is known to be 7–8 Å from where mannitol binds [12]. The same phosphorescence spectra and decay kinetics were observed for both proteins and it was concluded that the microenvironment of IIC^{mtl} near position 97 is not influenced by the cytoplasmic A and B domains.

4.3. Microenvironment of the 5-FTrp-labeled positions

Based on the λ^{max}, S–V and anisotropy data, none of the positions studied in this work show the characteristics typical for solvent exposed 5-FTrp residues. Except position 38, all studied positions are labeled with an aromatic amino acid in wt EII^{mtl}. Aromatic amino acids in membrane proteins are often located at the protein-lipid interface [42]. They may function as anchors to help stable embedding of the protein in the bilayer [43]. Trp- or 5-FTrp-fluorescence spectroscopy is an excellent tool to establish whether the side chain of Trp is at the surface or at a buried position. When surface-exposed, a high solvent accessibility for external quenchers is expected, as well as a red-shifted emission maximum and fast rotational dynamics of the indole side chain. The spectroscopic properties are not expected to be biased by the presence of the PEG-based $C_{10}E_5$ detergent, used to solubilize EII^{mtl}, as this detergent is known to cause only a modest blue shift of λ^{max}, does not reduce iodide accessibility significantly (Fig. S1), and causes only minimal restrictions on Trp side chain mobility (Fig. S2B). Taken together, the fluorescence data of the 13 studied positions in IIC^{mtl} do not correspond with the side chain of 5-FTrp exposed at the IIC^{mtl} surface.

In the ChbC structure most residue positions corresponding with the 5-FTrp-labeled positions in EII^{mtl} are at the protein surface, only the ChbC residues corresponding with positions 167 and 251 in EII^{mtl}, respectively, are at well-buried positions. For example, the fluorescence of mutant W327 with and without mannitol and W198 with mannitol was found essentially insensitive to KI as a quencher (Fig. 4). In the ChbC structure the corresponding residues, Ala409 and Ileu254, respectively [19], are at solvent-exposed positions. In contrast, Gly190, corresponding with position 167 in EII^{mtl}, is at a buried position in ChbC, while this work predicts residue 167 close to the protein surface. Thus the overall structure of EII^{mtl}, as studied in this work, is quite different from the reported ChbC structure. EII^{mtl} is a sugar transporter and large conformational changes may take place in the membrane-embedded C domain during the catalytic cycle, as also proposed for ChbC by Cao et al. [19]. The collected KI quenching data for W30 at 4 different stages of the transport cycle demonstrate this as the solvent accessibility increases significantly when the transporter proceeds from the unphosphorylated state without mannitol to phosphorylated EII^{mtl} in the presence of mannitol (Fig. 2A).

4.4. Structural organization of dimeric EII^{mtl}

In a recently published FRET study convincing evidence was presented that EII^{mtl} forms an asymmetric dimer, as the mannitol binding site was not found located symmetrically at the dimer interface of EII^{mtl} [12]. This study did not address which parts of EII^{mtl} differ in structure between the two protomers. The 5-FTrp fluorescence data in this manuscript shed light on this. In the mannitol bound state, (unphosphorylated) EII^{mtl} is expected to exist in one conformational state because the transporter binds mannitol with high affinity but cannot transport it. In the presence of mannitol six mutants show a fluorescence decay with a lifetime amplitude ratio of 50:50 or very close to this ratio (mutants W38, W42, W188, W198, W282, and W327) (Table 2). This 50:50 ratio likely reflects the presence of 5-FTrp embedded in different microenvironments at the two protomers of dimeric EII^{mtl}. The associated anisotropy decay spectrum of W66 and the blue shift in λ^{max} of W188, W198, and W260 upon KI titration (see above) also indicate structural differences between the two 5-FTrp per dimer in these mutants. These results therefore are in line with the previously made observation that the structure of the two EII^{mtl} protomers differs in the dimer. In dimeric ChbC, the structures of the two protomers are essentially the same showing this protein was crystallized in another conformation than EII^{mtl} as investigated in this study. The symmetry in ChbC might be a result of both binding sites being occupied by a sugar molecule while EII^{mtl}, as investigated in this work, binds only one mannitol molecule [7].

In summary, this fluorescence study has yielded site-specific structural information of 13 residue positions spread throughout the IIC^{mtl} domain at 2 to 4 stages of the transport cycle. We conclude that a large fraction of the IIC^{mtl} structure is involved in the transport cycle. This may be a common feature of the EII sugar transporters as the same was proposed for ChbC [19] after its 3D structure was solved.

Appendix A. Supplementary data

Supplementary data to this article can be found online at doi:10.1016/j.bbamem.2011.11.001.

References

[1] H. Nikaido, M.H. Saier, Transport proteins in bacteria—common themes in their design, Science 258 (1992) 936–942.
[2] G.T. Robillard, J. Broos, Structure/function studies on the bacterial carbohydrate transporters, enzymes II, of the phosphoenolpyruvate-dependent phosphotransferase system, Biochim. Biophys. Acta 1422 (1999) 73–104.
[3] J.W. Lengeler, K. Jahreis, U.F. Wehmeier, Enzymes II of the phospho enol pyruvate-dependent phosphotransferase systems: their structure and function in carbohydrate transport, Biochim. Biophys. Acta 1188 (1994) 1–28.
[4] R.L.M. van Montfort, T. Pijning, K.H. Kalk, I. Hangyi, M.L.C.E. Kouwijzer, G.T. Robillard, B.W. Dijkstra, The structure of the Escherichia coli phosphotransferase IIA(mannitol) reveals a novel fold with two conformations of the active site, Structure 6 (1998) 377–388.
[5] P.M. Legler, M.L. Cai, A. Peterkofsky, G.M. Clore, Three-dimensional solution structure of the cytoplasmic B domain of the mannitol transporter IIMannitol of the Escherichia coli phosphotransferase system, J. Biol. Chem. 279 (2004) 39115–39121.
[6] R.I. Koning, W. Keegstra, G.T. Oostergetel, G.K. Schuurman-Wolters, G.T. Robillard, A. Brisson, The 5 A projection structure of the transmembrane domain of the mannitol transporter enzyme II, J. Mol. Biol. 287 (1999) 845–851.
[7] G. Veldhuis, J. Broos, B. Poolman, R.M. Scheek, Stoichiometry and substrate affinity of the mannitol transporter, Enzymell(mtl), from *Escherichia coli*, Biophys. J. 89 (2005) 201–210.
[8] D. Swaving Dijkstra, J. Broos, J.S. Lolkema, H. Enequist, W. Minke, G.T. Robillard, A fluorescence study of single-tryptophan-containing mutants of enzyme II(mtl) of the *Escherichia coli* phosphoenolpyruvate-dependent mannitol transport system, Biochemistry 35 (1996) 6628–6634.
[9] D. Swaving Dijkstra, J. Broos, A.J. Visser, A. van Hoek, G.T. Robillard, Dynamic fluorescence spectroscopy on single tryptophan mutants of EII(mtl) in detergent micelles. Effects of substrate binding and phosphorylation on the fluorescence and anisotropy decay, Biochemistry 36 (1997) 4860–4866.
[10] J. Broos, F. ter Veld, G.T. Robillard, Membrane protein–ligand interactions in Escherichia coli vesicles and living cells monitored via a biosynthetically incorporated tryptophan analogue, Biochemistry 38 (1999) 9798–9803.
[11] E.P. Vos, M. Bokhove, B.H. Hesp, J. Broos, Structure of the cytoplasmic loop between putative helices II and III of the mannitol permease of *Escherichia coli*; a tryptophan and 5-fluorotryptophan spectroscopy study, Biochemistry 48 (2009) 5284–5290.
[12] M. Opacic, E.P. Vos, B.H. Hesp, J. Broos, Localization of the substrate binding site in the homodimeric mannitol transporter, EIImtl, of *Escherichia coli*, J. Biol. Chem. 285 (2010) 25324–25331.
[13] E.P. Vos, R. TerHorst, B. Poolman, J. Broos, Domain complementation studies reveal residues critical for the activity of the mannitol permease from *Escherichia coli*, Biochim. Biophys. Acta 1788 (2009) 581–586.
[14] J. Broos, F. Maddalena, B.H. Hesp, In vivo synthesized proteins with monoexponential fluorescence decay kinetics, J. Am. Chem. Soc. 126 (2004) 22–23.
[15] T.Q. Liu, P.R. Callis, B.H. Hesp, M. de Groot, W.J. Buma, J. Broos, Ionization potentials of fluoroindoles and the origin of nonexponential tryptophan fluorescence decay in proteins, J. Am. Chem. Soc. 127 (2005) 4104–4113.
[16] N.V. Visser, A.H. Westphal, S.M. Nabuurs, A. van Hoek, C.P.M. van Mierlo, A.J.W.G. Visser, J. Broos, H. van Amerongen, 5-Fluorotryptophan as dual probe for ground-state heterogeneity and excited-state dynamics in apoflavodoxin, FEBS Lett. 583 (2009) 2785–2788.
[17] R. Otten, F.S. van Lune, K. Dijkstra, R.M. Scheek, H-1, C-13, and N-15 resonance assignments of the phosphorylated enzyme IIB of the mannitol-specific phosphoenolpyruvate-dependent phosphotransferase system of *Escherichia coli*, J. Biomol. NMR 30 (2004) 461–462.
[18] J.Y. Suh, C. Tang, M.L. Cai, G.M. Clore, Visualization of the phosphorylated active site loop of the cytoplasmic B domain of the mannitol transporter IIMannitol of the *Escherichia coli* phosphotransferase system by NMR spectroscopy and residual dipolar couplings, J. Mol. Biol. 353 (2005) 1129–1136.
[19] Y. Cao, X.S. Jin, E.J. Levin, H. Huang, Y.N. Zong, M. Quick, J. Weng, Y.P. Pan, J. Love, M. Punta, B. Rost, W.A. Hendrickson, J.A. Javitch, K.R. Rajashankar, M. Zhou, Crystal structure of a phosphorylation-coupled saccharide transporter, Nature 473 (2011) 50–58.
[20] D. Swaving Dijkstra, J. Broos, G.T. Robillard, Membrane proteins and impure detergents: procedures to purify membrane proteins to a degree suitable for tryptophan fluorescence spectroscopy, Anal. Biochem. 240 (1996) 142–147.
[21] G. Veldhuis, E. Gabellieri, E.P.P. Vos, B. Poolman, G.B. Strambini, J. Broos, Substrate-induced conformational changes in the membrane-embedded IICmtl-domain of the mannitol permease from *Escherichia coli*, EnzymeII(mtl), probed by tryptophan phosphorescence spectroscopy, J. Biol. Chem. 280 (2005) 35148–35156.
[22] R.P. van Weeghel, Y.Y. van der Hoek, H.H. Pas, M. Elferink, W. Keck, G.T. Robillard, Details of mannitol transport in *Escherichia coli* elucidated by site-specific mutagenesis and complementation of phosphorylation site mutants of the phosphoenolpyruvate-dependent mannitol- specific phosphotransferase system, Biochemistry 30 (1991) 1768–1773.
[23] H. Boer, R.H. ten Hoeve Duurkens, J.S. Lolkema, G.T. Robillard, Phosphorylation site mutants of the mannitol transport protein enzyme IImtl of *Escherichia coli*: studies on the interaction between the mannitol translocating C-domain and the phosphorylation site on the energy-coupling B-domain, Biochemistry 34 (1995) 3239–3247.
[24] J. Broos, E. Gabellieri, E. Biemans-Oldehinkel, G.B. Strambini, Efficient biosynthetic incorporation of tryptophan and indole analogs in an integral membrane protein, Protein Sci. 12 (2003) 1991–2000.
[25] J. Broos, R.H. ten Hoeve Duurkens, G.T. Robillard, A mechanism to alter reversibly the oligomeric state of a membrane-bound protein demonstrated with *Escherichia coli* EII^{mtl} in solution, J. Biol. Chem. 273 (1998) 3865–3870.
[26] J.R. Lakowicz, Principles of Fluorescence Spectroscopy, Springer, New York, 2006.
[27] P. Cioni, G.B. Strambini, Acrylamide quenching of protein phosphorescence as a monitor of structural fluctuations in the globular fold, J. Am. Chem. Soc. 120 (1998) 11749–11757.
[28] L. Tortech, C. Jaxel, M. Vincent, J. Gallay, B. de Foresta, The polar headgroup of the detergent governs the accessibility to water of tryptophan octyl ester in host micelles, Biochim. Biophys. Acta-Biomembr. 1514 (2001) 76–86.
[29] Q.P. Weng, J. Elder, G.R. Jacobson, Site-specific mutagenesis of residues in the *Escherichia coli* mannitol permease that have been suggested to be important for its phosphorylation and chemoreception functions, J. Biol. Chem. 267 (1992) 19529–19535.
[30] C.A. Saraceni Richards, G.R. Jacobson, Subunit and amino acid interactions in the *Escherichia coli* mannitol permease: a functional complementation study of coexpressed mutant permease proteins, J. Bacteriol. 179 (1997) 5171–5177.
[31] C.A. Saraceni Richards, G.R. Jacobson, A conserved glutamate residue, Glu-257, is important for substrate binding and transport by the *Escherichia coli* mannitol permease, J. Bacteriol. 179 (1997) 1135–1142.
[32] H. Boer, R.H. ten Hoeve Duurkens, G.T. Robillard, Relation between the oligomerization state and the transport and phosphorylation function of the *Escherichia coli* mannitol transport protein: interaction between mannitol-specific enzyme II monomers studied by complementation of inactive site-directed mutants, Biochemistry 35 (1996) 12901–12908.
[33] S. Otte, A. Scholle, S. Turgut, J.W. Lengeler, Mutations which uncouple transport and phosphorylation in the D-mannitol phosphotransferase system of *Escherichia coli* K-12 and *Klebsiella pneumoniae* 1033-5P14, J. Bacteriol. 185 (2003) 2267–2276.
[34] J.W. Lengeler, F. Titgemeyer, A.P. Vogler, B.M. Wohrl, Structures and homologies of carbohydrate: phosphotransferase system (PTS) proteins, Philos. Trans. R. Soc. Lond. B Biol. Sci. 326 (1990) 489–504.
[35] T.X. Nguyen, M.R. Yen, R.D. Barabote, M.H. Saier, Topological predictions for integral membrane permeases of the phosphoenolpyruvate: sugar phosphotransferase system, J. Mol. Microbiol. Biotechnol. 11 (2006) 345–360.
[36] J.T. Vivian, P.R. Callis, Mechanisms of tryptophan fluorescence shifts in proteins, Biophys. J. 80 (2001) 2093–2109.
[37] J.S. Lolkema, R.H. ten Hoeve Duurkens, D. Swaving Dijkstra, G.T. Robillard, Mechanistic coupling of transport and phosphorylation activity by enzyme IImtl of the *Escherichia coli* phosphoenolpyruvate-dependent phosphotransferase system, Biochemistry 30 (1991) 6716–6721.
[38] M.G. Elferink, A.J. Driessen, G.T. Robillard, Functional reconstitution of the purified phosphoenolpyruvate-dependent mannitol-specific transport system of *Escherichia coli* in phospholipid vesicles: coupling between transport and phosphorylation, J. Bacteriol. 172 (1990) 7119–7125.
[39] W. Meijberg, G.K. Schuurman-Wolters, G.T. Robillard, Thermodynamic evidence for conformational coupling between the B and C domains of the mannitol transporter of *Escherichia coli*, Enzyme II^{mtl}, J. Biol. Chem. 273 (1998) 7949–7956.
[40] F.F. Roossien, G.T. Robillard, Vicinal dithiol-disulfide distribution in the *Escherichia coli* mannitol specific carrier enzyme IImtl, Biochemistry 23 (1984) 211–215.
[41] E.B. Vervoort, J.B. Bultema, G.K. Schuurman-Wolters, E.R. Geertsma, J. Broos, B. Poolman, The first cytoplasmic loop of the mannitol permease from *Escherichia coli* is accessible for sulfhydryl reagents from the periplasmic side of the membrane, J. Mol. Biol. 346 (2005) 733–743.
[42] L. Adamian, V. Nanda, W.F. DeGrado, J. Liang, Empirical lipid propensities of amino acid residues in multispan alpha helical membrane proteins, Proteins 59 (2005) 496–509.
[43] J.A. Killian, G. von Heijne, How proteins adapt to a membrane-water interface, Trends Biochem. Sci. 25 (2000) 429–434.